https://doi.org/10.2352/EI.2025.37.7.ISS-286
This work is licensed under the Creative Commons Attribution 4.0 International License.
To view a copy of this license, visit http://creativecommons.org/licenses/by/4.0/.

Optimization of polarization image sensor for electric field imaging system based on electro-optic effect

Kiyotaka Sasagawa[1,2], Ryoma Okada[1,2], Katsuya Hyodo[2], Hironari Takehara[2], Makito Haruta[3,4], Hiroyuki Tashiro[2,4], Jun Ohta[3];
[1]Medilux Research Center, Graduate School of Science and Technology, Nara Institute of Science and Technology; 8916-5 Takayama, Ikoma, Nara, Japan
[2]Division of Materials Science, Graduate School of Science and Technology, Nara Institute of Science and Technology; 8916-5 Takayama, Ikoma, Nara, Japan
[3]Institute for Research Initiatives, Nara Institute of Science and Technology; 8916-5 Takayama, Ikoma, Nara, Japan
[4]Department of Opto-Electronic System Engineering, Faculty of Science and Engineering, Chitose Institute of Science and Technology, 758-65 Bibi, Chitose, Hokkaido, Japan
[5]Department of Health Sciences, Faculty of Medical Sciences, Kyushu University, 3-1-1 Maidashi, Higashi-Ku, Fukuoka, Japan

Abstract

In this study, we investigated the improvement of the characteristics of the pixels of a polarization image sensor used for high-frequency electric field imaging. It was confirmed that the signal-to-noise ratio can be improved by increasing the number of metal wiring layers constituting the polarizer and by expanding the pixel dimensions. The combination of these improvements is expected to enable high-frequency field imaging with higher sensitivity.

Introduction

The electric field measurement technique using the electro-optic (EO) effect [1-3] is applicable to high frequencies up to THz, and when combined with image sensors, it is expected to be used for RF device evaluation [4-11] and inspection using THz waves [12-16]. However, the sensitivity of this method is low, and it requires significant improvement for practical applications. To solve this problem, we have developed a method to improve sensitivity using a polarization image sensor of our own design [17-22]. This has enabled the image sensor to measure electric fields in the frequency domain instead of the conventional time domain measurement, making it possible to image the response of a specific frequency in a short period of time.

However, the current system is only capable of measuring high-frequency electric fields of relatively high intensity, such as the near-field of a high-frequency device, and further improvement in sensitivity is needed. There remains room for improvement in image sensors as well, and improvements in pixels and readout circuits are required.

Objective

Based on the process limitations in polarized image sensor design, it is necessary to optimize for field imaging. There are several factors involved in optimization, including the configuration of the polarizer on the pixel, pixel capacitance, and inter-pixel crosstalk. The objective of this study is to find the optimal conditions for these from a prototype test pixel.

Method

Figure 1 shows the configuration of the optical system in a high-frequency field imaging system. In this configuration, a polarization image sensor is used as the image sensor. In electric field imaging, it is necessary to acquire faint changes. However,

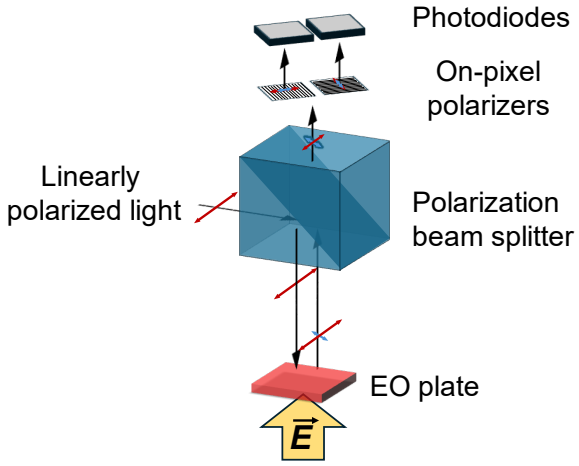

Figure 1. Optical setup of electro-optic imaging system

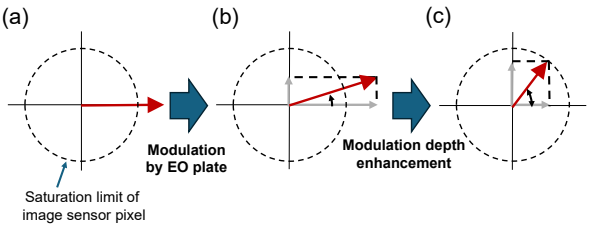

Figure 2. Polarization conditions at each point in the optical setup. (a) incident linear polarized light. (b) Polarization modulated light by the electrooptic crystal. (c) Modulation depth enhanced light through the PBS.

image sensor pixels generally have an upper limit on the signal-to-noise ratio due to photon shot noise and pixel saturation. In this configuration, the polarization beam splitter (PBS) and the on-pixel polarizer of the polarization image sensor form a dual-polarizer configuration. The on-pixel polarizers are arranged at 0 and 90 degrees, while the PBS is oriented at 45 degrees to both.

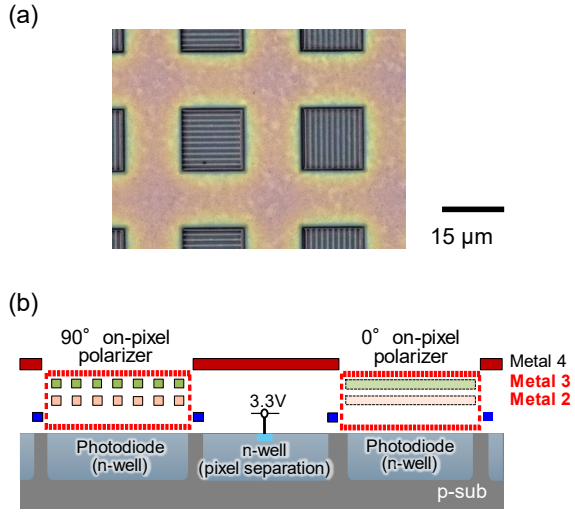

Figure 3. (a) Micrograph of 30- μ m polarization pixels. (b) Schematic of polarization pixel cross section.

TABLE I. Comparison of pixel specifications

	Previous work	This work
Pixel size	30 μm × 30 μm	45 μm × 45 μm
PD size	15 μm × 15 μm	33 μm × 33 μm
Fill factor	25%	53%
On-pixel polarizer	2 layers	3 layers
Extinction ratio	3.1	5.7

In the electric-field imaging systems based on the EO effect, the birefringence change induced on an EO crystal is read using light. Linearly polarized light is incident on the optical system. This light is of such high intensity that it would cause pixel saturation if it were irradiated directly onto the image sensor (Fig.2(a)). This polarization component is reflected by the PBS and irradiated to the EO crystal, which has an anti-reflection coating on the upper side and an high-reflection coating on the lower side, and travels back and forth within the crystal. The light returned to the PBS is mostly reflected. Here, the polarization of the light is modulated (Fig.2(b)) . An ideal polarizer transmits only one polarization component. However, as the practical PBS, a small portion of the incident polarization and most of the orthogonal polarization component are transmitted. This results in a reduction in light intensity and an increase in the depth of polarization modulation. (Fig.2(c)) This translates into a conversion of the signal to conditions that are easier to detect by the image sensor pixels.

In the practical experiment, the irradiated light is assumed to be intensity-modulated light. The modulation frequency f_{LO} is assumed to be a frequency slightly different from the frequency f RF of the high-frequency electric field to be observed. The combination of an EO crystal and a polarizer acts as a mixer, so the light detected by the pixel contains a component of intermediate frequency $f_{IF}=|f_{RF}-f_{LO}|$. The image sensor itself cannot detect the high-frequency signal of the observed object, but by setting f_{IF} to 1/4 of the frame rate, the intermediate frequency component including the electric field information of the observed object is detected.

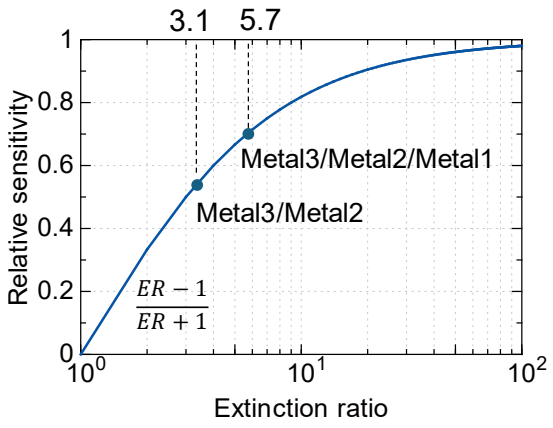

Figure 4. Relative sensitivity as a function of extinction ratio.

The incident light is at a wavelength of 780 nm. This wavelength is readily available for optical modulators and optical amplifiers and is also sufficiently detectable by Si image sensors. In particular, photodiodes using the n-well/p-sub structure of the 0.35-μm standard process used in this study have a relatively wide depletion layer and show sufficiently high sensitivity in this wavelength band. The pixel architecture is a 3-transistor active pixel sensor (APS). This is because the noise reduction effect using CDS by using 4-transistor APS was not expected to be significant in improving the characteristics for the purpose of this study, since it is intended to be used in the photon shot noise-limited region. The basic pixel structure is shown in Figure 3(a). In this example, the pixel size is 30-μm square and the PD size is 15-μm square. Figure 3(b) shows the cross-sectional structure. A 0° or 90° polarizer is mounted on the photodiode using a wiring layer. In this example, the polarizer is composed of two layers of Metal2 and Metal3.

Previous research has shown that the highest polarization extinction ratio at this wavelength is achieved by using a grating structure with a line/space ratio of 0.7 μm / 0.7 μm for the polarizer on the pixel using a metal interconnect layer. The extinction ratio also changes as the number of grating layers is increased. We fabricated pixels with different numbers of grating layers and investigated the optimum conditions. In addition, polarization image sensors are equipped with polarizers in different directions for neighboring pixels. This allows changes in the polarization to be observed to be read as complementary signals. However, as crosstalk increases between pixels, the effective polarization extinction ratio decreases, and polarization detection performance is reduced. In this regard, we investigated the optimal conditions for test pixels with pixel dimensions of 45 μm and different photodiode spacing and area by creating a prototype test pixel.

A comparison table between the newly fabricated pixel and previous pixels is shown in Table I. While increasing the pixel dimensions, the fill factor is also increased. This was determined based on the results of the crosstalk evaluation described below. The number of metal wiring layers used for the polarizer has also been increased.

Results

As for the number of polarizer layers, it improves with increasing the number of layers. At a wavelength of 780 nm, a polarization extinction ratio of 5.7 was obtained with three layers,

compared to 3.2 with two layers. This result indicates that the performance index, which is 1 when the extinction ratio is infinite, increases significantly from 0.26 to 0.70. Here, the performance index is given by (ER-1)/(ER+1), where ER is the extinction ratio.

Figure 5. Signal, noise and signal-to-noise ratio of (a) 30-μm pixel and (b) 45-μm pixel.

On the other hand, since the transmittance drops to about half, the improvement is not very large when the irradiance is constant. However, since the irradiated light intensity in the assumed field imaging system can be amplified by a semiconductor optical amplifier or the like to compensate for the reduction in optical sensitivity, the improvement in sensitivity due to the improved extinction ratio will contribute significantly to the overall improvement of the system.

It was confirmed that photodiode spacing affects the reduction of effective extinction ratio due to crosstalk: when the spacing of photodiodes separated by guard rings with n-well layers is reduced from 25 μm to 10 μm, the reduction in polarization detection performance index due to the reduction of effective extinction ratio is about 10%. However, considering the reduction in sensitivity due to the decrease in fill factor, the effect of crosstalk is not dominant up to a photodiode spacing of about 12 μm for a pixel dimension of 45 μm.

The results of evaluating the signal and noise of each of the pixels used in the previous study and those used in the current study are shown in Figure 5. The signal-to-noise ratios are also shown in these figures.

There is no significant difference in signal sensitivity. The increase in pixel dimensions increases the fill factor, although the sensitivity to the same number of photons is reduced due to the increase in pixel capacitance. As a result, no significant difference appears. On the other hand, noise is low. This result can be explained by the increase in pixel capacity. In both pixels, the noise component gradually increases with light intensity, indicating that the effect of photon shot noise increases with light intensity. However, in the 45 μm pixel, there is a small amount of readout noise influence even near pixel saturation.

The signal-to-noise ratio improved by roughly 4 dB over the entire observation area.Ideally, an improvement in SNR with an increase in fill factor near pixel saturation would have been expected, but the prototype pixel did not show that level of improvement. The effect of readout noise was negligible up to a PD size of 15 μm, but for further improvement at 45-μm pixels, it is necessary to consider methods to reduce readout noise such as CDS.

Conclusion

In this study, we investigated the optimization of polarization image sensor pixels for high-frequency field imaging using the EO effect. The extinction ratio was improved by a factor of 1.6 by using a three-layered polarizer. This contributes to a 4 dB increase in sensitivity when the amount of light reaching the PD is the same. In addition, an SNR improvement of about 4 dB was obtained for a pixel using a 45-μm pixel. With these improvements, it is estimated that the field detection sensitivity can be improved by approximately 8 dB.

Funding

This work was funded by the SCOPE project of the Ministry of Internal Affairs and Communications of Japan (Grant Number JP225007001).

Acknowledgment

The LSI design was carried out in collaboration with the d.lab-VDEC at The University of Tokyo and with Cadence Design Systems and Siemens Electronic Design Automation Japan K.K.

References

[1] J. A. Valdmanis *et al.*, "Picosecond electro-optic sampling system," Appl. Phys. Lett., vol. 41, no. 3, pp. 211‑212, 1982.

[2] J. A. Valdmanis *et al.*, "Subpicosecond electrical sampling," IEEE J. Quantum Electron., vol. 19, no. 4, pp. 664‑667,1983.

[3] K. J. Weingarten *et al.*, "Picosecond optical sampling of GaAs integrated circuits," IEEE J. Quantum Electron., vol. 24, no. 2, pp. 198-220, 1988.

[4] A. Sasaki *et al.*, "Electric-field scanning system using electro-optic sensor," IEICE Trans. Electron., vol. 86-C, no.7, pp. 1345-1351, 2003.

[5] K. Sasagawa *et al.*, "Live electrooptic imaging system based on ultraparallel photonic heterodyne for microwave near fields," IEEE Trans. Microw. Theory Tech., vol. 55, no. 12, pp. 2782-2791, 2007.

[6] K. Sasagawa *et al.*, "Low noise and high frequency resolution electrooptic sensing of RF near-fields using an external optical

modulator," IEEE/OSA J. Lightwave Technol., vol. 26, no. 10, pp. 1242‑1248, 2008.

[7] K. Sasagawa *et al.*, "Real-time digital signal processing for live electro-optic imaging," Opt. Express, vol. 17, no. 18, pp. 15641-15651, 2009.

[8] M. Tsuchiya *et al.*, "Image and/or movie analyses of 100-GHz traveling waves on the basis of real-time observation with a live electrooptic imaging camera," *IEEE Trans. Microw. Theory Tech.*, vol. 57, no. 12, pp. 3373‑3379, 2009.

[9] A. Kanno *et al.*, "Real-time visualization of electromagnetic waves propagating in air using live electro-optic imaging technique," Opt. Express, vol. 18, no. 10, pp. 10029-10035, 2010.

[10] M. Tsuchiya, "Live electrooptic imaging of W-band waves," *IEEE T. Microw. Theory Tech.*, vol. 58, no. 11, pp. 3011-3021, 2010.

[11] M. Tsuchiya *et al.*, "Nanoscopic live electrooptic imaging," Sci. Rep. vol. 11, 5541, 2021.

[12] Q. Wu *et al.*, "Two-dimensional electro-optic imaging of THz beams," Appl. Phys. Lett., vol. 69, no. 8, pp. 1026‑1028, 1996.

[13] F. Miyamaru *et al.*, "Terahertz two-dimensional electrooptic sampling using high speed complementary metal-oxide semiconductor camera," Jpn. J. Appl. Phys., vol. 43, no. 4A, L489‑L491, 2004.

[14] F. Blanchard *et al.*, "Real-time, subwavelength terahertz imaging," Ann. Rev. Mater. Res., vol. 43, no. 1, pp. 237‑259, 2013.

[15] S. Hisatake *et al.*, "Visualization of the spatial–temporal evolution of continuous electromagnetic waves in the terahertz range based on photonics technology," Optica, vol. 1, no. 6, pp. 365‑371, 2014.

[16] F. Blanchard *et al.*, "Real-time megapixel electro-optical imaging of THz beams with probe power normalization," Sensors, vol. 22, no. 12, 4482, 2022.

[17] R. Okada *et al.*, "A polarisation-analysing CMOS image sensor for sensitive polarisation modulation detection," Electron. Lett., vol. 57, no. 12, pp. 472-474, 2021.

[18] K. Sasagawa *et al.*, "Polarization image sensor for highly sensitive polarization modulation imaging based on stacked polarizers, " IEEE Trans. Electron Devices, vol. 69, no. 6, pp. 2924-2931, 2022.

[19] R. Okada *et al.*, "Improvement of on-pixel polarizer with 0.35 μm CMOS process for electro-optic imaging systems," Jpn. J. Appl. Phys., vol. 62, no. SC, SC1052, 2023.

[20] R. Okada *et al.*, "THz near-field intensity distribution imaging in 0.3-THz band using a highly sensitive polarization CMOS image sensor using a 0.35-μm CMOS process," Jpn. J. Appl. Phys., vol. 63, no. 3, 03SP66, 2024.

[21] R. Okada, *et al.*, "Performance improvement by multi-layer on-pixel polarizer structure using 0.35-μm CMOS process for high sensitivity electro-optic imaging system," SSDM2024, 2024, Himeji, 551

[22] Okada *et al.*, "Microwave electro-optical imaging system using a frequency tracking optical local oscillator source with a polarization CMOS image sensor," IEICE Electron. Express, vol. 22, 20240742, 2025. doi:10.1587/elex.22.20240742

Author Biography

Kiyotaka Sasagawa received his B.S. degree from Kyoto University in 1999 and his M.E. and Ph.D. degrees in materials science from NAIST, Japan, in 2001 and 2004, respectively. Subsequently, he became a researcher at the National Institute of Information and Communications Technology in Tokyo, Japan. In 2008, he joined NAIST, where he is currently a professor. His research interests include bioimaging, biosensing, and electromagnetic field imaging.

Ryoma Okada received his B.E. degree from Shizuoka University in 2020 and his M.E. and Ph.D. degrees in the Graduate School of Science and Technology from NAIST, Japan, in 2022 and 2024, respectively. He joined NAIST as an assistant professor in 2024. His current research interests include polarization image sensors and electromagnetic field imaging.

Katsuya Hyodo received his B.E. degree from Osaka University, Suita, Japan, in 2024. He is currently a master's course student at Nara Institute of Science and Technology. He is engaged in research on image sensors for high signal-to-noise ratio lock-in detection.

Hironari Takehara received his B.E. and M.E. in applied chemistry from Kansai University in 1984 and 1986 and a Ph.D. in materials science from NAIST in 2015. He worked as a semiconductor process engineer at Panasonic Corporation from 1986 to 2012, developing BiCMOS, high voltage SOI, and optoelectronic IC processes. He joined NAIST as a postdoctoral fellow in 2015 and became an assistant professor in 2019. Currently, he is the CEO of NAI.T.

Makito Haruta received his B.E. in bioscience and biotechnology from Okayama University in 2009 and his M.S. in biological science and Dr. Eng. in material science from NAIST in 2011 and 2014. He was a postdoctoral fellow at NAIST from 2014 to 2016. He joined NAIST as an assistant professor in 2016 and became an associate professor at Chitose Institute of Science and Technology in 2023.

Hiroyuki Tashiro received his B.E. and M.E. degrees in electrical and electronic engineering from Toyohashi University of Technology in 1994 and 1996 and his Ph.D. in engineering from NAIST in 2017. He worked at Nidek Co., Ltd. on ophthalmic surgical systems and retinal prostheses. He joined Kyushu University in 2004 as an assistant professor and became an adjunct associate professor at NAIST in 2019. His research focuses on artificial vision systems and neural interfaces.

Jun Ohta received his B.E., M.E., and Dr. Eng. degrees in applied physics from The University of Tokyo in 1981, 1983, and 1992. He joined Mitsubishi Electric Corporation in 1983 and was a visiting scientist at the University of Colorado, Boulder from 1992 to 1993. He joined NAIST in 1998 and became a professor in 2004. His research focuses on smart CMOS image sensors for biomedical applications and retinal prosthetic devices.

JOIN US AT THE NEXT EI!

electronic IMAGING

Imaging across applications . . . Where industry and academia meet!

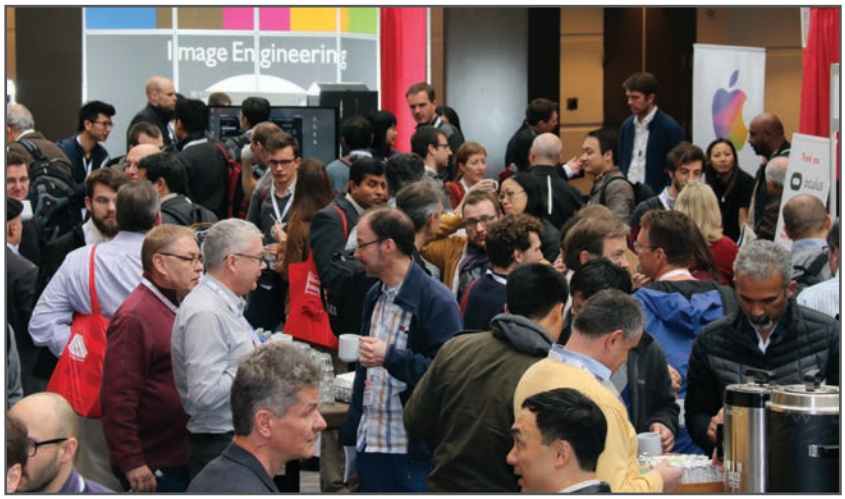

• SHORT COURSES • EXHIBITS • DEMONSTRATION SESSION • PLENARY TALKS •
• INTERACTIVE PAPER SESSION • SPECIAL EVENTS • TECHNICAL SESSIONS •

www.electronicimaging.org

ADVANCING IMAGING SCIENCE 75 1947 IS&T 2022 imaging.org